Adaptive Bandwidth Allocation in Multiuser MIMO THz Systems with Graph-Transformer Networks

Ali Mehrabian and Vincent W.S. Wong
Department of Electrical and Computer Engineering, The University of British Columbia, Vancouver, Canada
email: {alimehrabian619, vincentw}@ece.ubc.ca

***Abstract*—Terahertz (THz) wireless systems aim to support content-rich applications with ultra-high data rate. Due to high molecular absorption, THz signals experience severe path loss. Adaptive sub-band bandwidth (ASB) allocation can mitigate absorption attenuation by allocating THz sub-bands with variable bandwidth to the users. However, in ASB allocation, since the bandwidth of sub-bands may not be known *a priori*, accurate channel estimation is challenging. To overcome this issue, in this paper, we propose a heterogeneous graph-transformer network (HGTN) to bypass the channel estimation phase. We formulate a sum-rate maximization problem with quality-of-service (QoS) constraints in a multiuser multiple-input multiple-output (MU-MIMO) THz system to optimize the precoding and ASB allocation. The proposed HGTN parameterizes the mapping from input features (e.g., location information, users' minimum data rate) to the optimized system parameters via unsupervised learning. The proposed HGTN can be applied to systems with different number of users once it is trained. Simulation results show that our proposed HGTN achieves a higher system sum-rate with faster convergence when compared with the unsupervised deep neural network learning algorithm.**

I. Introduction

With the advancement of the sixth-generation (6G) systems, terahertz (THz) communication is envisioned as a promising solution to provide users with ultra-high throughput [1]. While the current fifth-generation (5G) systems can use millimeter-wave technology in the $30-300$ gigahertz (GHz) frequency range, the THz band spectrum range ($0.1-10$ THz) enables much higher data rate ranging from tens of gigabits to terabits per second and lower latency [2]. These advantages create a unique opportunity to advance the progress of many emerging applications, such as autonomous driving and extended reality. However, THz technology introduces previously unexplored challenges, which require novel approaches to address them.

For THz signals, in addition to the spreading loss and the higher channel sparsity, atmospheric absorption can significantly affect the propagation channel for users, which can lead to performance degradation. Specific frequencies in the THz band with the highest absorption of electromagnetic radiation are called molecular absorption coefficient peaks. They divide the THz spectrum into multiple ultra-wide THz transmission windows (TWs) [3]. The spectrum range of each TW is further divided into a set of sub-bands for allocation to the users. Due to the frequency-selective nature of THz signals, absorption loss variations within the sub-bands are high in different regions. As a result, new techniques need to be explored for THz spectrum management.

Recently, adaptive sub-band bandwidth (ASB) allocation has been proposed, in which the bandwidth allocated to each sub-band can be different. This approach can improve the spectral efficiency and mitigate the absorption loss. In [4], [5], joint sub-band assignment, ASB allocation, and power control is investigated in multi-connectivity THz systems. The authors considered single TW in [4] and multiple TWs in [5] to solve a sum-rate maximization problem using successive convex approximation. However, the joint use of multiple-input multiple-output (MIMO) technique and ASB allocation has not been investigated in [4], [5]. MIMO enables a large number of antennas to obtain a high directional gain and form narrow beams to separate users in the spatial domain [6]. As a result, precoding design in multiuser MIMO (MU-MIMO) THz systems would be beneficial to alleviate the absorption attenuation.

In THz systems, accurate channel estimation is a major issue. Pilot signal transmission in the THz band incurs a significant amount of system overhead due to a long training sequence transmission [7]. Moreover, in ASB allocation, the bandwidth within each sub-band is unknown in advance. This makes it challenging to determine the optimal duration and number of the pilot signals in the training sequence to capture the high variations of THz channel response for accurate channel estimation. In this paper, we aim to address the following question: *How should the base station (BS) optimize the adaptive bandwidth allocation and precoding in order to achieve a high system sum-rate without channel estimation?*

Recent works considered data-driven approaches to tackle the challenges of channel estimation. Since the channels in many wireless systems are largely functions of distance-dependent path loss [8], other available system information can be used to bypass the channel estimation phase. In particular, location information is utilized as input of deep neural networks (DNNs) for wireless link scheduling [8] and user association [9]. To determine the transmit power and ASB allocation in multiuser THz systems, the authors in [10] applied an unsupervised DNN using the distances between users and BS. However, DNNs do not comprehensively model the interaction between BS and users and require re-training for networks with different number of users.

To address the aforementioned issues, in this paper, we study ASB allocation with sub-band frequency reuse in a MU-MIMO THz system. We formulate an optimization problem for sum-rate maximization subject to the quality-of-service (QoS)

constraints by optimizing the precoding and ASB allocation. Obtaining the optimal solution of the formulated nonconvex problem with coupled optimization variables is challenging. Moreover, due to the high molecular absorption of the THz channel as well as the unknown bandwidth of THz sub-bands for ASB allocation, accurate channel estimation is challenging. To this end, we propose a heterogeneous graph-transformer network (HGTN) learning algorithm to solve the problem by bypassing the channel estimation phase. The main contributions of this paper are as follows:

- ***Heterogeneous Graph Representation***: We model the MU-MIMO THz system as a heterogeneous graph by defining the BS and users as two types of nodes. The input features of the node types include the location information and users' minimum data rate. We model the transmission links between nodes as graph edges. The graph structure is determined based on the distance information between the nodes.
- ***HGTN Distinct Advantages***: Our proposed HGTN can parameterize the mapping between the input features and system parameters using the information of graph nodes as well as structural information. Our end-to-end learning algorithm can bypass the channel estimation phase. It directly maps the input to the optimized system parameters via unsupervised training. Moreover, the parameter dimension of our learning algorithm is scalable. Once the network is trained, it can be applied in systems with different number of users.
- ***Performance Evaluation***: For a MU-MIMO THz system with six users, simulation results show that our proposed HGTN can achieve a system sum-rate that is 9.98% higher than that of unsupervised DNN learning algorithm [10]. Moreover, our proposed HGTN has faster training convergence compared to the baseline. We also show the performance gains obtained from using MIMO and ASB for improving the sum-rate in multiuser THz systems.

The remainder of this paper is organized as follows. The system model and problem formulation for MU-MIMO THz systems are described in Section II. In Section III, we present our proposed HGTN learning algorithm. Simulation results are presented in Section IV. Conclusions are given in Section V.

Notations: In this paper, we use $\mathbb{R}$ and $\mathbb{C}$ to denote the set of real and complex numbers, respectively. We use boldface upper-case letters (e.g., $\mathbf{X}$) to denote two-dimensional matrices or multi-dimensional tensors and boldface lower-case letters (e.g., $\mathbf{x}$) to denote vectors. $\mathbf{I}_N$ represents an $N \times N$ identity matrix. $(\cdot)^T$ and $(\cdot)^H$ denote the transpose and conjugate transpose of a vector or matrix, respectively. $\exp(\cdot)$ denotes the exponential function. j represents the imaginary unit satisfying $j^2 = -1$. $[\cdot]$ denotes the concatenate operation. $\text{tr}(\cdot)$ and $\det(\cdot)$ denote the trace and determinant of a matrix, respectively. $\|\cdot\|$ and $\|\cdot\|_F$ denote the norm of a vector and the Frobenius norm of a matrix, respectively. We denote the rectified linear unit function as $\text{ReLU}(x) = \max(x, 0)$. We denote the sigmoid function as $\sigma(x) = \frac{1}{1+\exp(-x)}$.

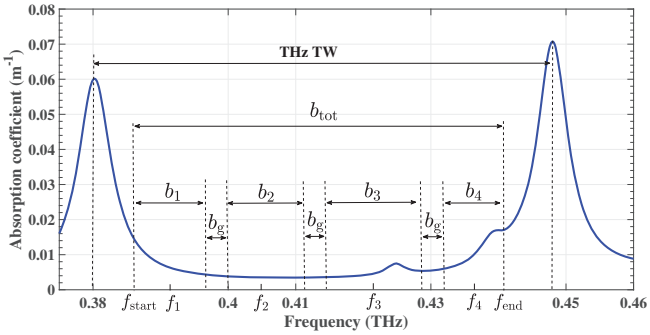

Fig. 1. Illustration of the molecular absorption coefficient $k_{\text{abs}}(f)$ and sub-band bandwidth allocation in a THz TW.

II. System Model and Problem Formulation

We consider a downlink MU-MIMO THz system, where the system has one BS to serve U users. Let $\mathcal{U} = \{1, \ldots, U\}$ denote the set of users. The BS is equipped with a uniform linear array (ULA) which has N_{t} antennas for THz signal transmission [2]. Each user is equipped with an N_{r}-element ULA antenna. As illustrated in Fig. 1, THz signals experience lower molecular absorption loss in a THz TW. In this paper, we consider non-overlapping ASB allocation in a TW, as shown in Fig. 1. Let $\mathcal{S} = \{1, 2, \ldots, S\}$ denote the set of sub-bands, where S is the total number of sub-bands. Let vectors $\mathbf{b} = (b_1, \ldots, b_S)$ and $\mathbf{f} = (f_1, \ldots, f_S)$ denote the bandwidth of the sub-bands and their central frequencies, respectively. Let $b_{\max}$ denote the maximum bandwidth of each sub-band. We have the following constraint for the bandwidth of each sub-band:

$$\text{C1}: \quad 0 \le b_s \le b_{\max}, \quad s \in \mathcal{S}. \tag{1}$$

Let f_{start} and f_{end} denote the start and end points of the spectrum region for bandwidth allocation, respectively. We consider b_{g} as the fixed guard band that separates the sub-bands to mitigate the inter-band interference [4], [5]. Let $b_{\text{tot}} = f_{\text{end}} - f_{\text{start}}$ denote the bandwidth of the spectrum region for allocation. We have the following constraint for the total available bandwidth:

$$\text{C2}: \quad \sum_{s \in \mathcal{S}} b_s = b_{\text{tot}} - (S-1) b_{\text{g}}. \tag{2}$$

The central frequency of sub-band $s \in \mathcal{S}$ can be represented as follows:

$$f_s = f_{\text{start}} + (s-1) b_{\text{g}} + \sum_{i=1}^{s-1} b_i + \frac{b_s}{2}, \quad s \in \mathcal{S}. \tag{3}$$

The signal transmission in the THz band tends to be highly directional and non-line-of-sight components are negligible [2]. As a result, we consider the line-of-sight (LoS) frequency-selective model for the communication channels. Let d_{Bu} denote the distance between user $u \in \mathcal{U}$ and BS. Let $\mathbf{H}_{Bu} \in \mathbb{C}^{N_{\text{r}} \times N_{\text{t}}}$ denote the BS-to-user u channel gains. They can be represented as follows:

$$\begin{aligned} \mathbf{H}_{Bu}(d, f) = & \sqrt{G_u G_B}\, \alpha\left(d_{Bu}, f\right) \\ & \mathbf{a}_u\left(\delta_{Bu}^A, \phi_{Bu}^A\right) \mathbf{a}_B^H\left(\delta_{Bu}^D, \phi_{Bu}^D\right), \end{aligned} \tag{4}$$

where G_u and G_B denote the antenna gains for user u and BS, respectively. $\left(\delta_{Bu}^A, \phi_{Bu}^A\right)$ are the azimuth and elevation angles of arrival for receiving signals and $\left(\delta_{Bu}^D, \phi_{Bu}^D\right)$ denote the azimuth and elevation angles of departure for transmitted signals in BS-to-user u transmissions, respectively. Moreover, $\mathbf{a}_u \in \mathbb{C}^{N_\mathrm{r}}$ and $\mathbf{a}_B \in \mathbb{C}^{N_\mathrm{t}}$ denote the array steering vectors for user u and BS, respectively. For $x \in \{1, \ldots, N_\mathrm{r}\}$ and $y \in \{1, \ldots, N_\mathrm{t}\}$, each element of the array steering vectors with angles (δ, ϕ) can be calculated as follows:

$$\mathbf{a}_u[x] = \frac{1}{\sqrt{N_\mathrm{r}}} \exp\left(j2\pi \frac{\epsilon_{\text{user}}}{\lambda}(x-1)\cos(\delta)\sin(\phi)\right), \quad \text{(5a)}$$

$$\mathbf{a}_B[y] = \frac{1}{\sqrt{N_\mathrm{t}}} \exp\left(j2\pi \frac{\epsilon_{\text{BS}}}{\lambda}(y-1)\cos(\delta)\sin(\phi)\right), \quad \text{(5b)}$$

where ϵ_{user} and ϵ_{BS} are antenna element spacing for a user and BS, respectively, and λ is the wavelength. The path loss factor $\alpha(d, f) \in \mathbb{R}$ with distance d between transmitter and receiver at frequency f can be calculated by $\alpha(d, f) = \left(\frac{c}{4\pi f d}\right) \exp\left(-\frac{1}{2} k_{\text{abs}}(f) d\right)$, where c is the speed of light, and $k_{\text{abs}}(f)$ is the molecular absorption coefficient which can be calculated by using the information from the HITRAN database [11], as illustrated in Fig. 1.

A. Achievable Data Rate

For the allocation of THz sub-bands to the users, we consider sub-band frequency reuse for users and the effect of intra-band interference. The achievable data rate (in bits/sec) for user $u \in \mathcal{U}$ using sub-band $s \in \mathcal{S}$ can be represented as [5]:

$$r_{u,s} = \int_{f_s - b_s/2}^{f_s + b_s/2} \log_2 \det \Bigg[\mathbf{I}_{N_\mathrm{r}} + \mathbf{\Gamma}_{u,s} \Big(N_0 b_s \mathbf{I}_{N_\mathrm{r}} + \sum_{i=1, i \neq u}^{U} \mathbf{\Gamma}_{i,s} \Big)^{-1} \Bigg] \mathrm{d}f, \quad (6)$$

where N_0 denotes the noise spectral density and f_s can be calculated by (3). The term $\mathbf{\Gamma}_{u,s} \in \mathbb{C}^{N_\mathrm{r} \times N_\mathrm{r}}$ for user u using sub-band s can be determined by $\mathbf{\Gamma}_{u,s} = \mathbf{H}_{Bu}(d_{Bu}, f)\mathbf{p}_{u,s}\mathbf{p}_{u,s}^H \mathbf{H}_{Bu}^H(d_{Bu}, f)$, where $\mathbf{p}_{u,s} \in \mathbb{C}^{N_\mathrm{t}}$ is the precoding vector for user u using sub-band s. We denote $\mathbf{P}_u \in \mathbb{C}^{S \times N_\mathrm{t}}$ as the precoding matrix for user u by considering all sub-bands and $\mathbf{P} = [\mathbf{P}_1, \ldots, \mathbf{P}_u, \ldots, \mathbf{P}_U] \in \mathbb{C}^{U \times S \times N_\mathrm{t}}$ as the precoder tensor at the BS, respectively. Since the rank of channel gain matrix $\mathbf{H}_{Bu}$ is equal to one, we consider a single data stream for signal transmission. The transmit power constraint is as follows:

$$\text{C3}: \sum_{u \in \mathcal{U}} \sum_{s \in \mathcal{S}} ||\mathbf{p}_{u,s}||_2^2 \leq P_{\max}, \quad (7)$$

where $P_{\max}$ denotes the maximum transmit power of the BS. To guarantee that the minimum data rate requirement of user u is satisfied, we have the following per-user QoS constraint:

$$\text{C4}: \sum_{s \in \mathcal{S}} r_{u,s} \geq r_{u,\min}, \quad u \in \mathcal{U}, \quad (8)$$

where $r_{u,\min}$ is the minimum required data rate of user u.

B. Problem Formulation

In this paper, we consider sum-rate maximization to jointly optimize the precoding matrices and THz sub-bands bandwidth allocation. We formulate the sum-rate maximization problem for a MU-MIMO THz system as follows:

$$\begin{aligned} \underset{\{\mathbf{P},\, \mathbf{b}\}}{\text{maximize}} \quad & \sum_{u \in \mathcal{U}} \sum_{s \in \mathcal{S}} r_{u,s} \\ \text{subject to} \quad & \text{constraints C1} - \text{C4}. \end{aligned} \quad (9)$$

Obtaining the optimal solution of formulated problem (9) is challenging due to the following reasons. First, problem (9) is nonconvex and the optimization variables are coupled. Second, calculating the objective function is difficult because the limits of the integration for determining $r_{u,s}$ depend on the optimization variable $\mathbf{b}$. Moreover, it is difficult to calculate the molecular absorption coefficient $k_{\text{abs}}(f)$ since there is no closed-form expression in terms of f for all spectrum regions in the THz band. As a result, there is no closed-form expression for $r_{u,s}$ in (6) as a function of sub-band bandwidth $\mathbf{b}$, which makes it difficult to solve the problem by using conventional optimization techniques. To this end, we propose a learning-based HGTN algorithm to solve problem (9).

III. HGTN Learning Algorithm

We first model the MU-MIMO THz system as a heterogeneous graph. Then, we develop an unsupervised HGTN learning algorithm to solve problem (9).

A. Graph Representation and Neighbour Feature Aggregation

We model the system as an undirected heterogeneous graph $\mathcal{G} = \{\mathcal{V}, \mathcal{E}, \Psi\}$. The graph consists of $U+1$ nodes, where the BS is represented by node v_B, and the U users are represented by nodes from v_1 to v_U. Let $\mathcal{V} = \{v_B, v_1, \ldots, v_U\}$ denote the set of nodes. We denote $\Psi = \{\psi_B, \psi_U\}$ as the set of node types, where ψ_B and ψ_U represent the BS and user node types, respectively. Let $\mathcal{E} = \{e_{mn} \mid v_m, v_n \in \mathcal{V}\}$ denote the set of edge weights, where $e_{mn} \in \mathbb{R}$ denotes the edge weight between nodes v_m and $v_n \in \mathcal{V}$. We consider a weighted cross-type connectivity matrix [12] and model the transmission links as graph edges between the graph nodes. To construct the weighted graph, we consider the distances between the graph nodes since the channel gain is a function of distance based on (4). Let $\mathbf{A} \in \mathbb{R}^{1 \times U}$ denote the cross-type connectivity matrix between BS and user node types. For user node $v_u \in \mathcal{V}$, the elements in the matrix between BS and users node types are $\mathbf{A}[1, u] = e_{Bu} = \frac{1}{d_{Bu}}$. We apply the softmax function to normalize the cross-type connectivity matrix as follows:

$$\hat{\mathbf{A}}[1, u] = \text{softmax}(\mathbf{A}[1, u]) = \frac{\exp(\mathbf{A}[1, u])}{\sum_{i=1}^{U} \exp(\mathbf{A}[1, i])}. \quad (10)$$

Moreover, each node type of the graph has a feature matrix. We use the location information of graph nodes and the users' minimum data rate to construct the feature matrices. To define the locations of nodes, we consider a three-dimensional (3-D) Cartesian coordinate system. Let $\mathbf{g}_u$ and $\mathbf{g}_B \in \mathbb{R}^3$ denote the geographical locations of user $u \in \mathcal{U}$ and BS, respectively. Let

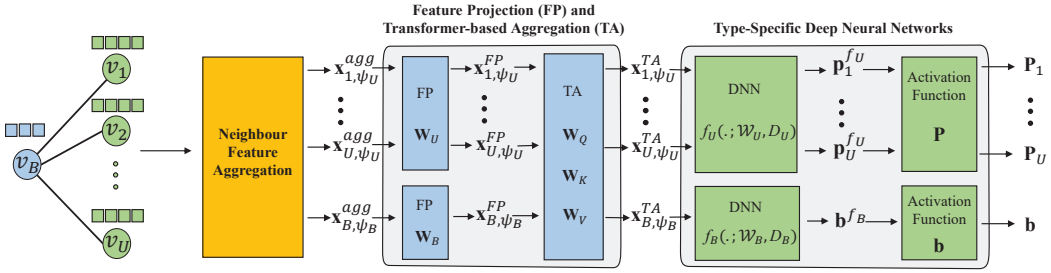

Fig. 2. The overall architecture of the proposed HGTN with heterogeneous graph $\mathcal{G}(\mathcal{V}, \mathcal{E}, \Psi)$ as input and system parameters $\{\mathbf{P}, \mathbf{b}\}$ as output.

$\mathbf{X}_{\psi_U} \in \mathbb{R}^{U\times 4}$ and $\mathbf{X}_{\psi_B} \in \mathbb{R}^{1\times 3}$ denote the feature matrices of user and BS node types, respectively. For each user node $v_u \in \mathcal{V}$ and BS node $v_B \in \mathcal{V}$, we define the feature matrices as $\mathbf{X}_{\psi_U}[u,:] = \left[\mathbf{g}_u^T, r_{u,\min}\right]$ and $\mathbf{X}_{\psi_B}[1,:] = [\mathbf{g}_B^T]$, respectively.

Motivated by [13], we propose a neighbour feature aggregation module, which uses the cross-type connectivity matrix to aggregate the feature information of user and BS node types. This weighted-mean feature aggregation module takes into account the structural information. We perform feature aggregation for user and BS node types as $\hat{\mathbf{X}}_{\psi_U} = \hat{\mathbf{A}}^T\mathbf{X}_{\psi_B}$ and $\hat{\mathbf{X}}_{\psi_B} = \hat{\mathbf{A}}\mathbf{X}_{\psi_U}$, respectively. Then, we encode the obtained features into one representation to define the aggregated feature vectors for user node $v_u \in \mathcal{V}$ and BS node $v_B \in \mathcal{V}$ as $\mathbf{x}_{u,\psi_U}^{agg} = \left([\hat{\mathbf{X}}_{\psi_U}, \mathbf{X}_{\psi_U}][u,:]\right)^T \in \mathbb{R}^7$ and $\mathbf{x}_{B,\psi_B}^{agg} = \left([\hat{\mathbf{X}}_{\psi_B}, \mathbf{X}_{\psi_B}][1,:]\right)^T \in \mathbb{R}^7$, respectively. Our proposed neighbour feature aggregation module is performed only once in the pre-training step and can be applied to large-scale graphs with low computational complexity.

B. Feature Projection and Transformer-based Aggregation

Since a heterogeneous graph has multiple node types, nodes can have feature information vectors with different dimensions and different contents (e.g., location information, users' minimum data rate). To this end, we apply a type-specific linear transformation for each node type to project the aggregated features into the same latent space. For the user node $v_u \in \mathcal{V}$ and BS node $v_B \in \mathcal{V}$, we have:

$$\mathbf{x}_{u,\psi_U}^{FP} = \mathbf{W}_U\mathbf{x}_{u,\psi_U}^{agg} + \mathbf{o}_U, \;\; \mathbf{x}_{B,\psi_B}^{FP} = \mathbf{W}_B\mathbf{x}_{B,\psi_B}^{agg} + \mathbf{o}_B, \quad (11)$$

where $\mathbf{W}_U, \mathbf{W}_B \in \mathbb{R}^{Z_{FP}\times 7}$, and $\mathbf{o}_U, \mathbf{o}_B \in \mathbb{R}^{Z_{FP}}$ are the learnable projection weights for user and BS node types, respectively, and Z_{FP} is a constant dimension.

To capture the mutual information of different node types, we leverage the self-attention mechanism [14]. In heterogeneous graphs, different nodes have different impacts on the feature information of other nodes. As a result, by using the self-attention mechanism, we assign different weights to different projected feature vectors. We first concatenate the projected feature vectors as matrix $\mathbf{X}^{FP} = \left[\mathbf{x}_{1,\psi_U}^{FP}, \ldots, \mathbf{x}_{U,\psi_U}^{FP}, \mathbf{x}_{B,\psi_B}^{FP}\right]^T \in \mathbb{R}^{(U+1)\times Z_{FP}}$. Then, for the projected feature vector $\mathbf{x}_m^{FP} = \left(\mathbf{X}^{FP}[m,:]\right)^T$ of each node $v_m \in \mathcal{V}$, we have:

$$\mathbf{q}_m = \mathbf{W}_Q\mathbf{x}_m^{FP}, \;\; \mathbf{k}_m = \mathbf{W}_K\mathbf{x}_m^{FP}, \;\; \mathbf{v}_m = \mathbf{W}_V\mathbf{x}_m^{FP}, \quad (12a)$$

$$\alpha_{mn} = \frac{\exp\left(\mathbf{q}_m^T\mathbf{k}_n\right)}{\sum_{v_t\in\mathcal{V}}\exp\left(\mathbf{q}_m^T\mathbf{k}_t\right)}, \;\; v_m, v_n \in \mathcal{V}, \quad (12b)$$

$$\mathbf{x}_m^{TA} = \beta\sum_{v_n\in\mathcal{V}}\alpha_{mn}\mathbf{v}_n + \mathbf{x}_m^{FP}, \;\; v_m \in \mathcal{V}, \quad (12c)$$

where $\mathbf{W}_Q, \mathbf{W}_K \in \mathbb{R}^{Z_{TA}\times Z_{FP}}$, $\mathbf{W}_V \in \mathbb{R}^{Z_{FP}\times Z_{FP}}$, and $\beta \in \mathbb{R}$ are the learnable parameters, and Z_{TA} is a constant dimension. Based on the obtained values, for each user node $v_u \in \mathcal{V}$, and BS node $v_B \in \mathcal{V}$, we construct embedding vectors $\mathbf{x}_{u,\psi_U}^{TA} = \mathbf{x}_u^{TA}$ and $\mathbf{x}_{B,\psi_B}^{TA} = \mathbf{x}_{U+1}^{TA}$, respectively. To obtain the target system parameters, the embeddings are used as input for the type-specific DNNs.

C. Type-Specific DNNs and Loss Function Design

In the final step, we propose two type-specific DNNs to determine the optimized system parameters for each node type while guaranteeing the constraints in problem (9). As illustrated in Fig. 2, the neural networks $f_U\left(\cdot; \mathcal{W}_U, D_U\right)$ and $f_B\left(\cdot; \mathcal{W}_B, D_B\right)$ are responsible for determining the precoding matrices and ASB allocation for user and BS node types, respectively. The last and the second last arguments of the neural networks denote the number of layers and the set of parameters for each neural network, respectively.

For the optimal precoding matrices, all the learnable parameters in the set $\mathcal{W}_U$ are initialized as complex values. We first feed the embedding vector $\mathbf{x}_{u,\psi_U}^{TA}$ of user node $v_u \in \mathcal{V}$ to the network with output vector $\mathbf{p}_u^{f_U} = f_U\left(\mathbf{x}_{u,\psi_U}^{TA}; \mathcal{W}_U, D_U\right) \in \mathbb{C}^{SN_t}$. To satisfy the transmit power constraint C3, the output matrix $\mathbf{P}^{f_U} = \left[\mathbf{p}_1^{f_U}, \ldots, \mathbf{p}_U^{f_U}\right]^T \in \mathbb{C}^{U\times SN_t}$ is fed through the activation function $\hat{\mathbf{P}} = \sqrt{P_{\max}}\mathbf{P}^{f_U}/\|\mathbf{P}^{f_U}\|_F$. Finally, based on the normalized values $\hat{\mathbf{p}}_u = (\hat{\mathbf{P}}[u,:])^T$ for each user, we construct the precoding matrix as follows:

$$\mathbf{P}_u = [\hat{\mathbf{p}}_u[1:S], \; \hat{\mathbf{p}}_u[S+1:2S], \; \ldots, \; \hat{\mathbf{p}}_u[S(N_t-1)+1:SN_t]], \;\; u \in \mathcal{U}. \quad (13)$$

During the learning procedure, all the user nodes share the same weights for feature projection, transformer-based aggregation module, as well as the same neural network architecture. As a result, once the proposed HGTN is trained, it can be applied to systems with different number of users.

For the optimal ASB allocation, the embedding vector $\mathbf{x}_{B,\psi_B}^{TA}$ of BS node $v_B \in \mathcal{V}$ is fed to the network with output vector $\mathbf{b}^{f_B} = f_B\left(\mathbf{x}_{B,\psi_B}^{TA}; \mathcal{W}_B, D_B\right) \in \mathbb{R}^S$. Next, to

satisfy constraints C1 and C2, we first normalize each element of the output vector $\mathbf{b}^{f_B}$ as $\hat{\mathbf{b}}[s] = \sigma(\mathbf{b}^{f_B}[s])(b_{\text{tot}} - (S-1)b_{\text{g}})/\sum_{s' \in \mathcal{S}} \sigma(\mathbf{b}^{f_B}[s'])$. Finally, to determine the sub-band bandwidth vector $\mathbf{b}$, we feed each element of the normalized vector $\hat{\mathbf{b}}$ to the activation function $\mathbf{b}[s] = b_{\max} - \text{ReLU}(b_{\max} - \hat{\mathbf{b}}[s])$, which ensures that each element is less than or equal to $b_{\max}$. During the learning procedure, constraint C1 is satisfied. The learning algorithm is trained in a way in order to fully utilize the available bandwidth to guarantee constraint C2.

We denote the set of all network parameters as $\mathbf{\Phi} = \{\mathbf{W}_U, \mathbf{o}_U, \mathbf{W}_B, \mathbf{o}_B, \mathbf{W}_Q, \mathbf{W}_K, \mathbf{W}_V, \beta, \mathcal{W}_U, \mathcal{W}_B\}$. The QoS constraint C4 is added to the objective function in problem (9) as a penalty term. To train the proposed HGTN, we adopt mini-batch gradient descent and define the loss function for each training epoch as follows:

$$\mathcal{L}_k(\mathbf{P}, \mathbf{b}; \mathbf{\Phi}) = \frac{1}{B} \sum_{i=1}^{B} \Bigg(- \sum_{u \in \mathcal{U}} \sum_{s \in \mathcal{S}} r_{u,s}(i) + \zeta_k \sum_{u \in \mathcal{U}} \text{ReLU}\Big(r_{u,\min} - \sum_{s \in \mathcal{S}} r_{u,s}(i) \Big) \Bigg), \quad k = 1, \ldots, K, \tag{14}$$

where $\mathcal{L}_k(\cdot)$ is the loss function of the k-th training epoch, B and K denote the size of the mini-batch and the number of epochs, and $r_{u,s}(i)$ is the data rate of user $u \in \mathcal{U}$ using sub-band $s \in \mathcal{S}$ for the i-th mini-batch sample. Moreover, the penalizing coefficient $\zeta_k \geq 0$ is updated as follows:

$$\zeta_{k+1} = \text{ReLU}\Bigg(\zeta_k + \frac{1}{B} \sum_{i=1}^{B} \sum_{u \in \mathcal{U}} \Big(r_{u,\min}(i) - \sum_{s \in \mathcal{S}} r_{u,s}(i) \Big) \Bigg). \tag{15}$$

The proposed HGTN is trained to minimize loss function (14) using Adam optimizer [15] in an unsupervised manner. Note that the channel model in (4) is only for generating training samples. Once the network has been trained at the BS, the locations and the users' minimum data rate are fed to the network to obtain the system parameters. The proposed HGTN learning algorithm is summarized in Algorithm 1.

Algorithm 1 Proposed HGTN Learning Algorithm

1: **Input**: Graph $\mathcal{G}(\mathcal{V}, \mathcal{E}, \Psi)$, feature matrices $\{\mathbf{X}_{\Psi_U}, \mathbf{X}_{\Psi_B}\}$, initialize network parameters $\mathbf{\Phi}$, mini-batch size B, number of training epochs K, initialize penalizing coefficient ζ_0.
2: Perform pre-training neighbor feature aggregation.
3: *Unsupervised Training*:
4: **for** each epoch **do**
5: Project the input features into the same latent space using (11).
6: Capture the mutual information of the node types and combine them by performing transformer-based aggregation using (12).
7: Calculate the loss function (14) by passing the embedding values of each node type to the designed DNNs $f_U(\cdot)$, $f_B(\cdot)$.
8: Update $\mathbf{\Phi}$ to minimize (14) using Adam optimizer [15].
9: Update penalizing coefficient using (15).
10: **end for**
11: **Training Output** Trained network with parameters $\mathbf{\Phi}$
12: *Testing Phase*:
13: Use the trained network with parameters $\mathbf{\Phi}$ to solve problem (9).
14: **Testing Output** System parameters $\{\mathbf{P}, \mathbf{b}\}$.

IV. Performance Evaluation

We simulate a MU-MIMO THz system where the (x, y, z)-coordinates of the BS location in meters is $(25, -20, -5)$. Six users are randomly and uniformly distributed within a rectangular area $[0, 15] \times [0, 25]$ in the (x, y)-plane with $z = -10$. The ULA of the BS and ULA for each user are configured parallel to the (y, z)-plane. As illustrated in Fig. 1, we consider the absorption coefficient values based on the HITRAN database [11] for the standard atmosphere with a water vapor density of $1.5\ g/m^3$ and $15°C$ temperature. Based on the system setting and simulation parameters in Table I, we generate 15,000 samples, where 12,000 samples are used for training, and the remaining 3,000 samples are used for testing. To implement the neural networks, we use the PyTorch library and Adam optimizer [15]. The initial learning rate is set to 10^{-4}. The constant dimensions Z_{FP} and Z_{TA} are 1024 and 256, respectively. We consider the fully connected networks in the final step with two layers, and the hidden dimension unit is similar to the output dimension for each network. The mini-batch size B and the number of training epochs K are set to 256 and 250, respectively. The initial penalizing coefficient ζ_0 is equal to 12×10^9. For performance comparison, we extend the unsupervised DNN learning algorithm in [10] for the MU-MIMO THz system to jointly optimize the precoding matrices and ASB allocation in problem (9).

TABLE I
List of Simulation Parameters

Parameters	Value	Parameters	Value
S	5	$f_{\text{start}} - f_{\text{end}}$	$0.38 - 0.4$ THz
$b_{\max},\ b_{\text{g}}$	4, 0.75 GHz [5]	N_0	-174 dBm/Hz [10]
$P_{\max}$	30 dBm	$r_{u,\min}$	13 Gbps
N_{t}	12	N_{r}	2
$G_B,\ G_u$	25, 15 dBi	$\epsilon_{\text{user}},\ \epsilon_{\text{BS}}$	$0.15\ \mu m$

We first investigate the convergence of our proposed HGTN. We show the system sum-rate of the HGTN and the baseline versus the number of training epochs in Fig. 3(a). Results show that our proposed HGTN learning algorithm has faster convergence. It provides a system sum-rate that is 9.98% higher than that of unsupervised DNN learning algorithm. Fig. 3(b) shows that the penalizing coefficient ζ_k in (15) converges to zero after 50 iterations, which implies that the QoS constraint C4 is satisfied.

To examine the impact of MIMO signal transmission, we plot the system sum-rate versus the number of antennas at the BS, N_{t}, in Fig. 4. We observe that increasing N_{t} improves the sum-rate for all the learning algorithms. This indicates that optimal precoding design can provide users with high data rates in THz systems. Moreover, Fig. 4 shows that the performance improvement of the MU-MIMO THz system with the proposed HGTN over the baseline scheme increases with the value of N_{t}. In particular, when N_{t} is equal to 16, the proposed HGTN achieves a system sum-rate that is 11.64% higher than that of DNN learning algorithm.

Finally, to study the impact of ASB allocation, we compare the system sum-rate by varying the maximum sub-band bandwidth $b_{\max}$. We also consider equal sub-band bandwidth (ESB) allocation with HGTN, in which sub-bands have equal

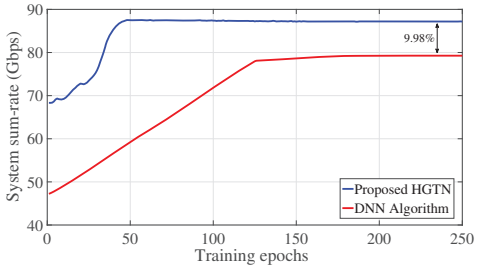

(a)

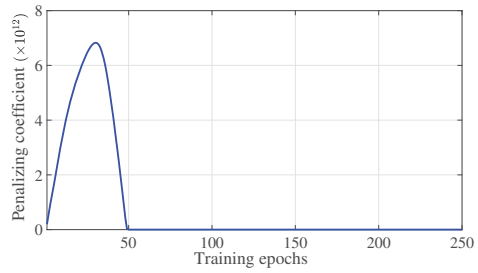

(b)

Fig. 3. (a) Convergence of the proposed HGTN and DNN learning algorithms. (b) Convergence of the penalizing coefficient ζ_k for the QoS constraint C4.

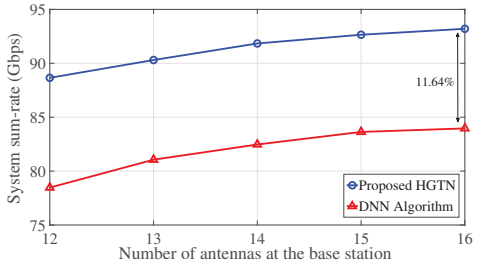

Fig. 4. System sum-rate versus the number of antennas N_{t} at the BS.

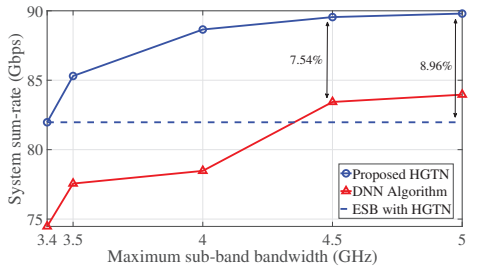

Fig. 5. System sum-rate versus the maximum sub-band bandwidth $b_{\max}$.

bandwidth (i.e., 3.4 GHz) and the precoding matrices are optimized by our proposed HGTN. In Fig. 5, by increasing $b_{\max}$, the system sum-rate for HGTN and DNN learning algorithms is improved. This is because larger $b_{\max}$ offers more flexibility for ASB allocation. Our proposed HGTN achieves an 8.96% higher system sum-rate compared to ESB allocation with HGTN. Additionally, by increasing $b_{\max}$, our proposed HGTN shows better performance compared to the DNN in terms of system sum-rate. In particular, when $b_{\max}$ is equal to 4.5 GHz, the proposed HGTN achieves a 7.54% higher system sum-rate compared to the DNN learning algorithm.

V. Conclusion

In this paper, we investigated the sum-rate maximization problem in MU-MIMO THz systems. We studied the joint optimization of precoding and ASB allocation. Since the THz sub-band bandwidth is not known beforehand in ASB allocation, accurate channel estimation is challenging. To overcome this issue, we proposed an unsupervised HGTN learning algorithm to solve the problem by bypassing the channel estimation phase. Through simulations, we showed that our proposed HGTN achieves a higher system sum-rate with faster convergence compared to the unsupervised DNN learning algorithm. We also demonstrated the system sum-rate improvements obtained from using MIMO and ASB in multiuser THz systems. In the journal version [16] of this work, we study ASB allocation in reconfigurable intelligent surface (RIS)-aided MU-MIMO THz systems.

References

[1] C.-X. Wang, J. Wang, S. Hu, Z. H. Jiang, J. Tao, and F. Yan, "Key technologies in 6G terahertz wireless communication systems: A survey," *IEEE Veh. Technol. Mag.*, vol. 16, no. 4, pp. 27–37, Dec. 2021.

[2] Z. Wan, Z. Gao, F. Gao, M. Di Renzo, and M.-S. Alouini, "Terahertz massive MIMO with holographic reconfigurable intelligent surfaces," *IEEE Trans. Commun.*, vol. 69, no. 7, pp. 4732–4750, Jul. 2021.

[3] I. F. Akyildiz, C. Han, Z. Hu, S. Nie, and J. M. Jornet, "Terahertz band communication: An old problem revisited and research directions for the next decade," *IEEE Trans. Commun.*, vol. 70, no. 6, pp. 4250–4285, Jun. 2022.

[4] A. Shafie, N. Yang, S. A. Alvi, C. Han, S. Durrani, and J. M. Jornet, "Spectrum allocation with adaptive sub-band bandwidth for terahertz communication systems," *IEEE Trans. Commun.*, vol. 70, no. 2, pp. 1407–1422, Feb. 2021.

[5] A. Shafie, N. Yang, C. Han, and J. M. Jornet, "Novel spectrum allocation among multiple transmission windows for terahertz communication systems," *IEEE Trans. Veh. Technol.*, vol. 71, no. 12, pp. 13 415–13 421, Dec. 2022.

[6] H. Sarieddeen, M.-S. Alouini, and T. Y. Al-Naffouri, "An overview of signal processing techniques for terahertz communications," *Proc. of the IEEE*, vol. 109, no. 10, pp. 1628–1665, Oct. 2021.

[7] V. Schram, A. Moldovan, and W. H. Gerstacker, "Compressive sensing for indoor THz channel estimation," in *Proc. of Asilomar Conf. on Sig., Syst., and Comput.*, Pacific Grove, CA, Oct. 2018.

[8] W. Cui, K. Shen, and W. Yu, "Spatial deep learning for wireless scheduling," *IEEE J. Sel. Areas Commun.*, vol. 37, no. 6, pp. 1248–1261, Jun. 2019.

[9] R. Liu, M. Lee, G. Yu, and G. Y. Li, "User association for millimeter-wave networks: A machine learning approach," *IEEE Trans. Commun.*, vol. 68, no. 7, pp. 4162–4174, Jul. 2020.

[10] A. Shafie, C. Lit, N. Yang, X. Zhou, and T. Q. Duong, "An unsupervised learning approach for spectrum allocation in terahertz communication systems," in *Proc. of IEEE Global Commun. Conf. (GLOBECOM)*, Rio de Janeiro, Brazil, Dec. 2022.

[11] E. A. L. S. Rothman, "The HITRAN 2008 molecular spectroscopic database," *J. Quant. Spectrosc. Radiat. Transf.*, vol. 110, no. 9-10, pp. 533–572, Jun. 2009.

[12] A. Mehrabian, S. Bahrami, and V. W.S. Wong, "A dynamic Bernstein graph recurrent network for wireless cellular traffic prediction," in *Proc. of IEEE Int. Conf. Commun. (ICC)*, Rome, Italy, May 2023.

[13] X. Yang, M. Yan, S. Pan, X. Ye, and D. Fan, "Simple and efficient heterogeneous graph neural network," in *Proc. of AAAI Conf. on Artif. Intell.*, Washington, DC, Feb. 2023.

[14] A. Vaswani, N. Shazeer, N. Parmar, J. Uszkoreit, L. Jones, A. N. Gomez, Ł. Kaiser, and I. Polosukhin, "Attention is all you need," in *Proc. Advances in Neural Inf. Process. Syst. (NeurIPS)*, Long Beach, CA, Dec. 2017.

[15] D. P. Kingma and J. Ba, "Adam: A method for stochastic optimization," in *Proc. Int'l Conf. Learn. Representations (ICLR)*, San Diego, CA, May 2015.

[16] A. Mehrabian and V. W. S. Wong, "Joint spectrum, precoding, and phase shifts design for RIS-aided multiuser MIMO THz systems," accepted for publication in *IEEE Trans. Commun.*, 2024.